A Comparison of MGMR3D and CoREAS Simulations for Four-layer Atmospheric Electric Field Structures

Trinh Thi Ngoc Gia[1,*], Nguyen Duy Sang[2], Pham Van Tuan[3]

Use your smartphone to scan this QR code and download this article

[1]*Department of Physics Education, School of Education, Can Tho University, Campus II, 3/2 Street, Ninh Kieu Ward, Can Tho 94000, Vietnam*

[2]*Department of Mathematics and Informatics Education, School of Education, Can Tho University, Campus II, 3/2 Street, Ninh Kieu Ward, Can Tho 94000, Vietnam*

[3]*Can Tho University Elite High School, Can Tho University, Campus II, 3/2 Street, Ninh Kieu Ward, Can Tho 94000, Vietnam*

Correspondence

Trinh Thi Ngoc Gia, Department of Physics Education, School of Education, Can Tho University, Campus II, 3/2 Street, Ninh Kieu Ward, Can Tho 94000, Vietnam
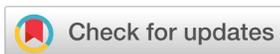
Email: ttngia@ctu.edu.vn

Check for updates

ABSTRACT

Introduction: Radio emissions from extensive air showers can provide valuable insights into the properties of high-energy cosmic rays and the atmospheric conditions through which they propagate. While these emissions can be accurately modeled under fair-weather conditions, the presence of strong and complex atmospheric electric fields during thunderstorms can significantly affect the radio signal. Methods: Measuring these fields directly is challenging due to the instability and unpredictability of thunderclouds, making indirect methods essential. The macroscopic model MGMR3D (Macroscopic GeoMagnetic Radiation, three-dimensional model) offers a semi-analytic approach to reconstructing these atmospheric electric field structures, while the microscopic simulation CoREAS (CORSIKA-based Radio Emission from Air Showers) serves as a detailed benchmark. In this study, the outputs of MGMR3D were validated against CoREAS to assess its ability to reproduce radio emission patterns under multi-layer thunderstorm field configurations. Both models were used to determine the intensity, linear polarization, and circular polarization of radio emissions generated by extensive air showers as they traversed layered electric field structures, including complex four-layer models. Results: The comparison demonstrated that MGMR3D can reliably reproduce the results obtained from CoREAS for both simple electric field configurations as well as intricate four-layer structures. The good agreement between both models indicates that MGMR3D captures the essential physics governing radio emission in strong electric field conditions. Conclusion: The findings demonstrate that MGMR3D, through its optimization procedure, is an efficient tool for reconstructing the internal electric field structures of thunderclouds; consequently, the model is suitable for extracting detailed electric field profiles from experimental radio measurements. This represents an important step in the use of radio detection as a diagnostic tool for atmospheric electricity during thunderstorms.

Key words: atmospheric electric fields, extensive air showers, radio emission models

INTRODUCTION

High-energy cosmic rays that enter the Earth's atmosphere can collide with oxygen or nitrogen nuclei to produce cascades of secondary particles, resulting in the formation of extensive air showers (EAS). These showers propagate toward the ground at nearly the speed of light. The number of particles in the shower increases until it reaches a maximum before decreasing when the particle energies become too low to sustain further multiplication. The atmospheric depth at which this maximum occurs is denoted as Xmax.

Due to the geomagnetic field, electrons and positrons in the shower are deflected in opposite directions by the Lorentz force. This creates a transverse current perpendicular to the shower axis that produces radio emissions that are polarized along the direction of the Lorentz force. In addition, the shower front carries an excess of electrons relative to positrons, resulting in a net negative charge that gives rise to another component of the radio emission. This so-called charge-excess radiation is linearly polarized radially with respect to the shower axis[1-3].

The intense atmospheric electric fields present in thunderclouds can influence the trajectory of shower particles. Indeed, the polarization and intensity footprints of the radio signal from these particles deviate significantly from those observed under fair-weather conditions. Consequently, measurements of EAS radio emission obtained during thunderstorms can be used to gain insights into the structure of electric fields within thunderclouds. Achieving this requires models that can accurately reproduce the underlying radio-emission mechanisms[4,5].

Two microscopic approaches are available for this purpose: **ZHAireS** and **CoREAS** (the latter implemented as a plug-in for the shower simulation code **CORSIKA**)[6-9]. In CORSIKA, extensive air showers can be simulated in the presence of atmospheric electric fields by activating the EFIELD option. Both microscopic models compute the resultant radio signal

by summing the contributions of individual charged particles; the trajectory of each particle is divided into small segments, and the radiation emitted by each segment is evaluated.

In contrast to microscopic approaches, **MGMR3D** is a macroscopic model that computes the radiation field directly from the Liénard–Wiechert potentials by parameterizing the four-current of the shower. MGMR3D is computationally much faster than CoREAS, making it suitable for optimization procedures aimed at reconstructing atmospheric electric fields from radio data. Previous studies have shown that results generated from MGMR3D and CoREAS are consistent for two- and three-layer electric field configurations. However, some air-shower events cannot be reproduced within the three-layer framework: more complex field structures are required to describe such cases. Furthermore, observations indicate that thunderclouds can occasionally exhibit four-layer electric fields [10,11].

This work extends previous studies by investigating radio emissions from the propagation of EAS through four-layer electric field structures using MGMR3D calculations and comparing the results to CoREAS simulations.

METHODS

This section outlines the theoretical framework and simulation procedures used to assess MGMR3D's ability to reproduce radio emissions from extensive air showers under thunderstorm conditions. The aim is to determine how accurately this macroscopic model can reconstruct complex four-layer atmospheric electric field configurations when compared with the microscopic simulations conducted by CoREAS.

Under thunderstorm conditions, the strong electric fields present in thunderclouds act in conjunction with the Lorentz force on charged particles within extensive air showers. These fields can be decomposed into two components: parallel and perpendicular to the shower axis. The parallel component either increases or decreases the number of electrons and positrons depending on its direction; however, the additional particles produced are typically low-energy and lag far behind the shower front, so their radiation does not significantly contribute to the 30–80 MHz frequency band of interest. Consequently, the contribution of the parallel component is set to zero in our analysis. In contrast, the perpendicular component does not change the particle number but instead modifies both the magnitude and direction of the transverse current. Consequently, it influences not only the

intensity but also the polarization of the radio emission.

The MGMR3D model is an analytic framework that computes the radio footprint of EAS directly from Maxwell's equations, using a parameterized description of the current density. This parameterization is informed by detailed microscopic shower simulations, with particular emphasis on the role of atmospheric electric fields [12,13]. Unlike Monte Carlo approaches, MGMR3D offers high computational efficiency and can be run using relatively modest resources.

To assess the accuracy of MGMR3D in modeling four-layer electric field configurations, we compared its predicted radio footprints with those obtained from CoREAS simulations. Here, air showers propagate through an atmosphere divided into four distinct electric field layers. Each layer i is defined by the altitude of its upper boundary (h_i), as well as the magnitude and orientation of the electric field within that layer. The layers are indexed sequentially from 1 to 4.

The radio signal of each shower is sampled with a star-shaped antenna array centered on the shower axis. The layout comprises eight radial arms: each arm contains 20 antennas along the shower plane that are separated by 25 m intervals. The recorded pulses are bandpass-filtered to the 30–80 MHz range. To fit both the intensity and polarization footprints simultaneously, the real-valued Stokes parameters are calculated at every antenna position. These parameters are defined as follows:

$$I = \frac{1}{n} \sum_{i=0}^{n-1} \left(\left| \varepsilon_{i,v \times B} \right|^2 + \left| \varepsilon_{i,v \times (v \times B)} \right|^2 \right),$$

$$Q = \frac{1}{n} \sum_{i=0}^{n-1} \left(\left| \varepsilon_{i,v \times B} \right|^2 + \left| \varepsilon_{i,v \times (v \times B)} \right|^2 \right),$$

$$U + iV = \frac{2}{n} \sum_{i=0}^{n-1} \left(\varepsilon_{i,v \times B} \varepsilon_{i,v \times (v \times B)}^* \right),$$

where v denotes the direction of the air shower, **B** is the geomagnetic field, and ε_i is the complex-valued signal radiation field, where i denotes the sample number. The sampling rate is 2×10^8 samples per second. The radiation fields were reconstructed from the recorded voltages by inverting the antenna calibration. Summation was performed over $n = 11$ samples, centered around the peak of the pulse. Stokes I corresponds to the total intensity of the radio emission, Stokes V represents the circular polarization, while Stokes Q and U can be combined to determine the linear polarization angle as follows:

$$\psi = \frac{1}{2} \tan^{-1} \left(\frac{U}{Q} \right)$$

To evaluate the performance of MGMR3D, simulations were conducted using different values of χ_{max} ranging between 600–900 g/cm^2 in steps of 20 g/cm^2. For each fixed Xmax, 12 parameters describing the

four-layer electric field structure were fitted. The goodness-of-fit was quantified using the reduced chi-squared statistic:

$$\chi^2 = \sum_{antenna\ j} \sum_{S=I,Q,U}^{V} \left(\frac{S_{j,CoREAS} - f S_{j,MGMR3D}}{\sigma_j} \right)^2 ,$$

where f is the normalization factor and σ_j denotes the uncertainties.

Finally, the simulation yielding the smallest reduced χ^2 was selected, and the corresponding fitted electric field configuration was compared to the input fields used in the CoREAS simulation.

RESULTS

Figure 1 presents the comparison between the Stokes parameters obtained from the CoREAS and MGMR3D simulations for Sample 1. The lower panels describe the residuals between the two sets of results, with σ indicating one standard deviation. The corresponding electric field parameters and χ_{max} are presented in Table 1.

Figure 1 shows that MGMR3D was highly consistent with the CoREAS results. Specifically, the radio-intensity footprint (left panel) exhibited a pronounced maximum at the shower core as well a distinct ring-like structure approximately 175 m in diameter. Strong linear and circular polarization features can be observed; these can only be accounted for by the rotation of the electric field between successive layers. In particular, the sign change of the circular polarization—from positive to negative with increasing distance from the shower axis—occurs due to the rotation of the electric field from 45° in layer 4 to 180° in layer 3 and back to 90° in layer 2.

Table 1 shows that both models contain four electric field layers and that the χ_{max} value obtained from MGMR3D differs from the value obtained from CoREAS by 25 g/cm^2. The difference in altitude in the three lower layers was less than 0.3 km, while the discrepancy in the upper layer was much higher at 0.7 km. At this altitude, the shower is still young and contains fewer particles; consequently, the radio emissions generated from this layer contribute very little to the total radio signal, making it difficult to accurately reconstruct its height. The strengths of the electric fields were also highly consistent, with only a difference of 5 kV/m. The directions of the electric fields in all layers were also well-reproduced, with less than a 5° difference compared to the CoREAS values.

Figure 2 presents the Stokes parameters derived from the MGMR3D and CoREAS models for Sample 2. The left panel shows the intensity profile, which again peaks at the shower core and exhibits a ring-like structure approximately 175 m from the core. The ring-like

structure is the result of interference between emissions from different layers. The circular polarization shown in the right panel of Figure 2 changes sign at a distance of about 150 m from the shower core, reflecting a reversal in the rotation direction of the electric fields, and thus the transverse current, between layers. The two middle panels illustrate how linear polarization varies with distance from the core. In general, the CoREAS simulations and MGMR3D calculations for Sample 2 agree closely; the discrepancies are smaller than two standard deviations.

Table 2 presents the twelve parameters used to characterize the electric field, as well as the χ_{max} values used in the CoREAS simulation and obtained from the MGMR3D calculation. The χ_{max} values were found to differ by 13 g/cm^2, which is less than the average uncertainty of χ_{max}. The electric field structure obtained from MGMR3D contains four layers, and the discrepancies in the heights of these layers compared to CoREAS were less than 0.2 km, except for the top height, which differed by 0.4 km. As mentioned previously, the shower is still young at this altitude and contains fewer particles, reducing its contribution to the radio signal. The electric field strengths obtained from MGMR3D were in close agreement with the CoREAS values in all four layers, while the reconstructed directions were nearly identical for both models.

DISCUSSION

The intensity footprints of both samples exhibit a peak at the shower core as well as ring-like structures; these structures are usually observed in the showers measured under thunderstorm conditions due to the changes in the direction of electric fields under these conditions. This results in constructive and destructive interference between the radio emissions from different layers.

The values of Stokes Q in Samples 1 and 2 are negative and positive, respectively, because the electric fields in the two lowest layers in Sample 2 are almost perpendicular to those in Sample 1. The linear polarization in Sample 2 aligns with the **vxB**-direction near the core of the shower but rotates toward an angle of around 50° relative to the **vxB**-direction at larger distances. At these larger distances, the antennas receive signals from high altitudes. In the second layer (4–5 km), the electric field is strong and oriented 45° to the **vxB**-direction. In contrast, the angle of linear polarization is more stable in Sample 1.

In Sample 1, the amount of circular polarization decreases gradually with increasing distance along the shower axis because the electric fields rotate gradually
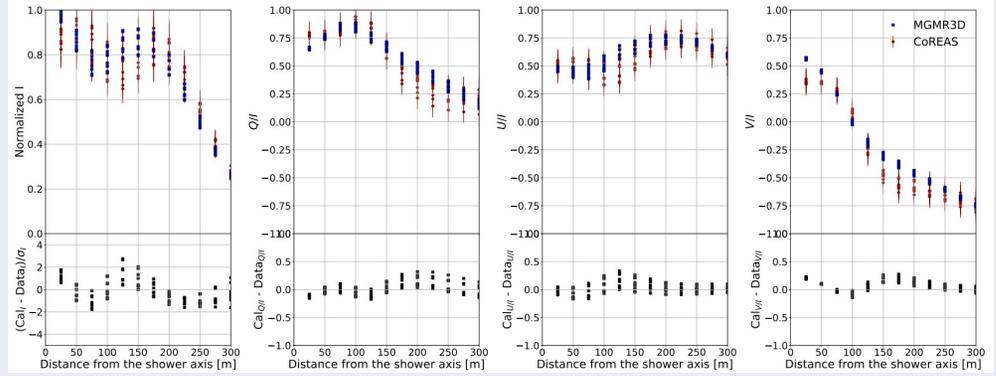
Figure 1: The MGMR3D results for the Stokes parameters (blue dots) compared to those obtained from CoREAS (red circles) for Sample 1. Error bars indicate one standard deviation σ.

Table 1: The twelve fitted electric field parameters and χ_{max} for Sample 1.

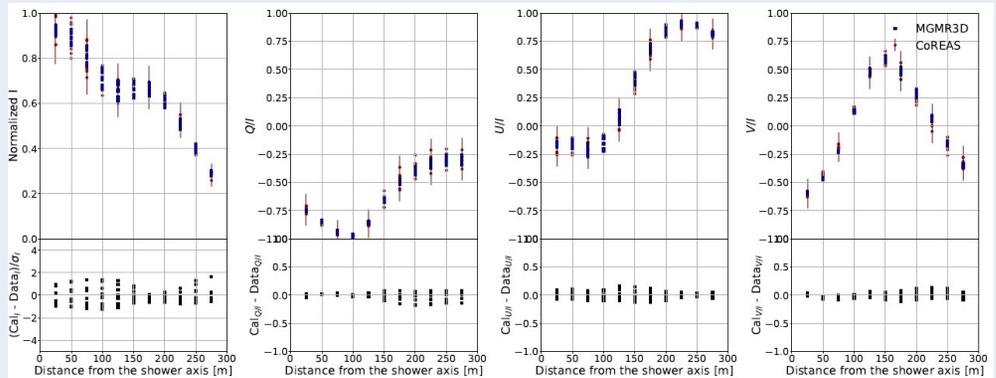| Layer	h [km]		E [kV/m]		$\alpha[^0]$	
	CoREAS	MGMR3D	CoREAS	MGMR3D	CoREAS	MGMR3D
1	8.0	8.7	30	32	45	48
2	6.0	5.8	50	55	90	91
3	4.0	3.9	40	45	180	182
4	2.0	1.9	20	23	45	40
$\chi_{maxCoREAS}$ [g/cm^2]	650					
$\chi_{maxMGMR3D}$ [g/cm^2]	675					

Figure 2: The MGMR3D results for the Stokes parameters (blue dots) compared with those obtained from CoREAS (red circles) for Sample 2. Error bars indicate one standard deviation σ

Table 2: The twelve fitted electric field parameters and χ_{max} for Sample 2.

Layer	h [km]		E [kV/m]		$\alpha[^0]$	
	CoREAS	MGMR3D	CoREAS	MGMR3D	CoREAS	MGMR3D
1	8.0	8.4	75	70	20	22
2	5.0	4.9	100	90	55	54
3	4.0	3.8	50	54	-90	-93
4	2.0	1.9	15	18	-45	-40
$\chi_{maxCoREAS}$ [g/cm^2]	634					
$\chi_{maxMGMR3D}$ [g/cm^2]	621					

from 45° to 90°, then 180°, and back to 45°. In contrast, the circular polarization of Sample 2 increases to about 0.75 at 150 m and then decreases at large distances from the core of the shower; this behavior is caused by an almost inverted electric field between the second (~4 km) and third layers.

The comparison between CoREAS and MGMR3D for both samples shows that the largest discrepancy concerns the height of the uppermost layer. At high altitudes, the shower is still in its early stages and contains relatively few particles; consequently, the radio emissions from these regions are weak, and the reconstruction of the corresponding electric field parameters is much less sensitive to the height of this layer. In contrast, the reconstructed heights of the three lower layers differ by less than 0.2 km, indicating that they can be determined with higher reliability. Furthermore, both models agree closely on the strength and orientation of the electric fields in all layers.

CONCLUSIONS

Radio emissions from EAS are influenced by the electric fields in thunderclouds. Both macroscopic and microscopic models are used to simulate these electric fields. In this study, the emissions predicted by CoREAS in four-layer electric field configurations were compared with those obtained from the macroscopic MGMR3D model. The results show that there is a reduced sensitivity to the height of the uppermost layer, where the shower is still relatively young. Aside from this constraint, however, results from MGMR3D are strongly consistent with those from CoREAS, demonstrating its suitability for inferring electric field structures from measured radio signals.

ABBREVIATIONS

MGMR3D: Macroscopic GeoMagnetic Radiation, three-dimensional model

CoREAS: CORSIKA-based Radio Emission from Air Showers

Xmax: Atmospheric depth at which the number of shower particles reaches its maximum

COMPETING INTERESTS

The authors declare that they have no competing interests.

AUTHORS' CONTRIBUTIONS

Trinh Thi Ngoc Gia: Investigation, analyzing, reviewing and editing.
Nguyen Duy Sang: analyzing, reviewing and editing.
Pham Van Tuan: Investigation and reviewing.

ACKNOWLEDGEMENTS

REFERENCES

1. Scholten O, Werner K, Rusydi F. A macroscopic description of coherent geo-magnetic radiation from cosmic-ray air showers. Astropart Phys. 2008;29(2):94–103. Available from: https://doi.org/10.1016/j.astropartphys.2007.11.012.

2. Werner K, de Vries KD, Scholten O. A realistic treatment of geomagnetic Cherenkov radiation from cosmic ray air showers. Astropart Phys. 2012;37:5–16. Available from: https://doi.org/10.1016/j.astropartphys.2012.07.007.

3. Scholten O, Werner K. Macroscopic model of geomagnetic-radiation from air showers, Nucl. Instrum. Methods Phys. Res. Sect A. 2009;604:24.

4. Schellart P, Trinh TN, Buitink S, Corstanje A, Enriquez JE, Falcke H, et al. Probing Atmospheric Electric Fields in Thunderstorms through Radio Emission from Cosmic-Ray-Induced Air Showers. Phys Rev Lett. 2015;114(16). Available from: https://doi.org/10.1103/PhysRevLett.114.165001.

5. Trinh TN, Scholten O, Buitink S, van den Berg AM, Corstanje A, Ebert U, et al. Influence of atmospheric electric fields on the radio emission from extensive air showers. Phys Rev D. 2016;93(2). Available from: https://doi.org/10.1103/PhysRevD.93.023003.

6. Alvarez-Muñiz J, Jr WR. Monte Carlo simulations of radio pulses in atmospheric showers using ZHAireS. Astropart Phys. 2012;35(6):325–41. Available from: https://doi.org/10.1016/j.astropartphys.2011.10.005.

7. Huege T, Ludwig M, James CW. Simulating radio emission from air showers with coreas. AIP Conf Proc. 2013;1535:128–32. Available from: https://doi.org/10.1063/1.4807534.

8. Heck D. CORSIKA: a Monte Carlo Code to Simulate Extensive Air Showers. Hannover: TIB Hannover; 1998.

9. Buitink S, Apel WD, Asch T, Badea F, Bähren L, Bekk K, et al. Amplified radio emission from cosmic ray air showers in thunderstorms. Astron Astrophys. 2007;467(2):385–94. Available from: https://doi.org/10.1051/0004-6361:20066006.

10. Scholten O, Trinh TN, de Vries KD, Hare BM. Analytic calculation of radio emission from parametrized extensive air showers: A tool to extract shower parameters. Phys Rev D. 2018;97(2). Available from: https://doi.org/10.1103/PhysRevD.97.023005.

11. Trinh TN, Scholten O, Buitink S, de Vries KD, Mitra P, Nguyen TP, et al. Determine atmospheric electric fields using MGMR3D. Phys Rev D. 2022;105(6). Available from: https://doi.org/10.1103/PhysRevD.105.063027.